

## Multichannel resonance processes: Theory and application to the Auger spectra of the CO molecule

Renato Colle

*Dipartimento di Chimica Applicata, Facoltà di Ingegneria, Università di Bologna-Viale Risorgimento 2, 40136 Bologna, Italy  
and Scuola Normale Superiore, Piazza dei Cavalieri 7, 56126 Pisa, Italy*

Stefano Simonucci

*Dipartimento di Matematica e Fisica, Università di Camerino, Via Madonna delle Carceri 7, Camerino, Italy  
(Received 18 January 1993)*

A general expression for predicting vibrational profiles of a molecular Auger spectrum is derived. The relationship between a “theoretical” cross section and an experimental spectrum is discussed and specific procedures for implementing cross-section calculations in the Born-Oppenheimer approximation are proposed. The carbon and oxygen *K*-*LL* Auger spectra of CO are reproduced on the entire energy range of interest and specific spectral regions are analyzed in greater detail. The results are compared with experimental data.

PACS number(s): 31.15.+q, 33.10.-n, 33.70.Jg, 33.80.Eh

### I. INTRODUCTION

High-resolution electron spectroscopies involving core electrons are becoming more and more available both in molecular and in solid-state physics [1–4]. This fact makes it possible to resolve—both in emission and in absorption spectra—fine-structure details which are due to the nuclear motion, thus providing a fundamental contribution to the understanding of the electronic and vibrational structure of various systems.

Among these spectroscopies, those involving emission or excitation of core electrons—such as Auger or autoionization—are of special interest when applied to molecules since, in this case, the vibrational effects do not merely produce a broadening of the observed bands, but quite often introduce asymmetric and complicated structures due to the combined effects of different intermediate and final states. The key point that characterizes the Auger and autoionization processes is, in fact, the presence of short-lived intermediate states which are, in the molecular context, vibronic levels belonging to the core-hole states produced in the initial ionization process. These levels are populated with different probabilities and decay with different lifetimes to final vibronic states which are grouped in various vibrational progressions often overlapping because of small spacings among the electronic states.

All of these facts, on the one hand, confirm the importance of having a clear theoretical instrument with which to interpret the molecular Auger spectra, an instrument that should necessarily take into account the effects of the nuclear motion for rationalizing the fine-structure details and the distinct features of these spectra. On the other hand, one can understand why very few detailed theoretical studies have been carried out in molecules, when one realizes the difficulties associated with a quantitative, nonempirical prediction of the characteristic features of these spectra, namely position, width, intensity and shape

of the bands on an energy range of the order of 50–100 eV.

The great majority of these studies analyze the Auger spectra only in terms of vertical electronic transitions [5–8], while a few of them construct the vibrational profile of selected bands [9,10] or use approximate techniques for reproducing the main features of the whole spectrum [11–13]—see Ref. [14] for a general overview. Almost all the authors who calculate the vibrational structure of a given electronic band make use of the same approximate equation, derived by different authors in various contexts [15–17,10]. This formula, when applied to the vibronic profile of a given band—e.g., that relative to the electronic state  $|f\rangle$ —can be written as follows:

$$\sigma_f(E) \propto \sum_{n_f} \left| \sum_{n_c} \frac{\langle 0 | \hat{V}' | n_c \rangle \langle n_c | \hat{V} | n_f \rangle}{E - (E_{n_c} - E_{n_f}) - i\Gamma_{n_c}/2} \right|^2, \quad (1)$$

where  $|0\rangle$  represents the ground vibrational state of the neutral molecule,  $\{|n_c\rangle\}$  are the intermediate vibrational states of the core-ionized molecule, each with energy  $E_{n_c}$  and linewidth  $\Gamma_{n_c}$ , and  $\hat{V}'$  and  $\hat{V}$  are the coupling operators that govern the transitions, respectively, from the ground to the intermediate and from the intermediate to the final vibronic states  $\{|n_f\rangle\}$  having energies  $\{E_{n_f}\}$ . In the specific molecular applications of Eq. (1) the dependence of  $\hat{V}$  and  $\hat{V}'$  on the internuclear coordinates is usually ignored (“crude adiabatic” approximation) and the lifetime of the intermediate states is assumed independent of the energy and the internuclear dynamics (“constant-resonance-width” approximation), thereby  $\Gamma_{n_c} \sim \Gamma$ . Note that by applying these approximations to Eq. (1) one gets a simplified expression that can equivalently be derived also from a time-dependent formulation of the problem and which has been used for estimating “center of gravity” and width of the bands—see

Refs. [9,11].

The aim of this paper is to derive a general expression for predicting the experimental profile of a given molecular Auger spectrum without introducing any specific assumption either on the number or type of the resonances or on the internuclear coordinate dependence of the wave functions and spectral parameters that are involved. To this end we have applied Fano's theory [18] for the interaction among a number of discrete states and several continua since, using this scheme, one obtains a simple expression for the cross section of each decay process that can be analyzed in its different physical contributions. By estimating the relative importance of these contributions one can also introduce the approximations necessary to simplify the computational problem and produce a working equation that is more general than Eq. (1) and does not require the use of non-Hermitian operators with complex, energy-dependent, nonlocal potentials such as that proposed in Ref. [10].

The method presented in this paper is the generalization—to include the vibrational effects—of the approach recently proposed by us [12,13] for the study of the electronic decay processes in molecules. This approach allows one to obtain the electronic quantities—such as continuum wave functions, energy shifts, linewidths, etc.—that are implied in the calculation of the vibrational cross sections and that determine, through their dependence on the internuclear coordinates, the spectral profile of the various bands.

In Sec. II A we derive a general expression for the cross section of an Auger decay process. In Sec. II B we propose a procedure for constructing the discrete and continuum functions and for calculating the matrix elements that are involved in the cross-section calculations. This procedure makes use of the Born-Oppenheimer (BO) approximation, an assumption that is quite appropriate in usual cases where both the intermediate and the final electronic states of the ionized molecule are well separated in energy.

In Sec. III we apply our method to the calculation of the carbon and oxygen *K-LL* Auger spectra of CO, a molecule for which accurate experimental results [9,19–21] and several theoretical investigations [8,9,11,22,23] are available. Carbon monoxide has been chosen since its Auger spectrum presents very distinct features that constitute a crucial test of any theoretical method. Previous calculations on this molecule either reproduce a few vibrational progressions by fitting energy shifts and total intensities to the experimental data [9] or give the global spectral profile but neglect the fine-structure details [11].

Using our *ab initio* approach we reproduce not only the experimental profile of the whole spectrum by convoluting the various band profiles with a spectrometer broadening function, but we give also the details of the vibrational structure underlying the experimental spectrum over the entire energy range of interest. Furthermore, by enlarging the energy scale, we analyze the details of a few interesting spectral regions and relate their main features to the nuclear coordinate dependence of the matrix elements implied in the calculation of the

spectral parameters and to the form of the potential-energy surfaces that govern the decay process.

## II. THEORY

It is well established that the Auger process can be studied as a multichannel resonant scattering process in which the intermediate states are bound states of the core-ionized molecule embedded in continua that are open channels classified according to the state of the doubly ionized molecule and to the kinetic energy of the Auger electron. This model is based on the assumption that the primary photoelectron carries enough energy to prevent any appreciable post-collisional interaction with the core-ionized molecule, an assumption that is quite reasonable because, in a typical Auger experiment, the energy of the photon that produces the primary ionization is much bigger than the kinetic energy of the emitted Auger electron.

Starting from this assumption and making use of a time-independent scheme, one can reasonably approximate the state vector for the  $N$ -electron molecule as an antisymmetrized product of two strong-orthogonal vectors, i.e.,  $|\Psi^N\rangle = \hat{\mathcal{A}}[|\Psi^{N-1}\rangle|\eta_{\epsilon_1}\rangle]$ , where  $|\Psi^{N-1}\rangle$  represents a possible state of the  $(N-1)$ -electron system,  $|\eta_{\epsilon_1}\rangle$  one of the primary photoelectrons and  $\hat{\mathcal{A}}$  is the operator that antisymmetrizes the state and includes the normalization constant. The problem is thereby reduced to the determination of the eigenstates of the Hamiltonian ( $\hat{H}^{N-1}$ ) of the  $(N-1)$ -electron system at energies near the resonances. The latter, in a molecular Auger problem, correspond to rotovibrational levels pertaining to the electronic core-hole state(s) produced in the initial ionization process. Note that, in principle, one should consider the rotovibrational levels of the molecule, since the emission cross section is relative to transitions between states that are classified according to their electronic, vibrational, and rotational quantum numbers. However, due to the finite-resolution power of the spectrometer, it is reasonable to ignore the details of the rotational structure and assume, as we did in the specific applications of our method, that only one rotational level is populated for each electronic and vibrational state, and precisely that level which has the highest probability of occupation at room temperature and according to the Boltzmann distribution function.

### A. A general expression for the cross section of an Auger decay process

In order to construct the eigenfunctions of the molecular Hamiltonian describing the electronic and nuclear motion of the  $(N-1)$ -electron system, we follow the time-independent approach proposed by Fano [18] to treat the case of a number ( $m_d$ ) of discrete states  $\{\Phi_j\}$  interacting with several ( $m_c$ ) continua  $\{\chi_{\beta,\mathbf{k}}\}$ . We use the formalism of Refs. [12,13] and impose the ingoing wave boundary condition “(–)” on the continuum functions. This choice derives from the fact that we are interested in a problem where the electron is released from within the scatterer and travels away from the doubly ionized mole-

cule following a specific direction ( $\mathbf{k}$ ) and with a specific kinetic energy ( $\varepsilon = \frac{1}{2}k^2$ ). In our approximate treatment—see Refs. [12,13]—the long-range potential that governs the dynamic of the Auger electron is well reproduced inside the molecular volume, but reduces to the centrifugal potential outside this region. Because of this fact we can use the wave vector  $\mathbf{k}$  as a good quantum number in the asymptotic limit and define the corresponding behavior of the continuum function as follows:

$$\lim_{r \rightarrow \infty} \chi_{\beta, \mathbf{k}}^- = \sum_{\gamma} \Omega_{\gamma} \left[ e^{ik_{\gamma} r} \delta_{\gamma\beta} - \frac{e^{-ik_{\gamma} r}}{2ikr} f_{\gamma\beta}(\hat{\mathbf{r}}, \hat{\mathbf{k}}_{\gamma}) \right]. \quad (2)$$

In Eq. (2) the symmetry-adapted wave function  $\Omega_{\gamma}$  represents an electronic and vibrational state of the doubly ionized molecule and  $f_{\gamma\beta}(\hat{\mathbf{r}}, \hat{\mathbf{k}}_{\gamma})$  gives the probability amplitude of channel  $\gamma$ .

Let us now construct the eigenfunction  $\Psi_{\text{ap}}^-$  of  $H^{N-1}$  at the energy  $E = E_{\alpha} + \frac{1}{2}p^2$ , which is the sum of the energies of the two separate fragments, i.e., of the doubly ionized molecule in the state  $|\alpha\rangle$  and of the Auger electron having asymptotically energy  $\varepsilon = \frac{1}{2}p^2$ . This eigenfunction, which satisfies the “ingoing-wave” boundary condition, can be expressed in terms of the discrete intermediate states  $\{\Phi_j\}$  and of the decay channels  $\{\chi_{\beta, \mathbf{k}}\}$  as follows:

$$\Psi_{\text{ap}}^- = \sum_{j=1}^{m_d} \Phi_j a_{j\alpha}(\mathbf{p}) + \sum_{\beta=1}^{m_c} \int \frac{d\mathbf{k}}{(2\pi)^3} \chi_{\beta\mathbf{k}}^- b_{\beta\alpha}(\mathbf{k}, \mathbf{p}), \quad (3)$$

with the normalization condition

$$\langle \Psi_{\beta\mathbf{k}}^- | \Psi_{\text{ap}}^- \rangle = \delta_{\beta\alpha} (2\pi)^3 \delta(\mathbf{k} - \mathbf{p}). \quad (4)$$

The elements of the Hamiltonian matrix constructed using the discrete and continuum wave functions are as follows:

$$\langle \Phi_l | \hat{H} - E | \Phi_j \rangle = (E_l - E) \delta_{lj}, \quad (5)$$

$$\langle \chi_{\gamma\tau}^- | \hat{H} - E | \chi_{\beta\mathbf{k}}^- \rangle = \left[ E_{\gamma} + \frac{\tau^2}{2} - E \right] \delta_{\gamma\beta} (2\pi)^3 \delta(\tau - \mathbf{k}), \quad (6)$$

$$\langle \Phi_l | \hat{H} - E | \chi_{\beta\mathbf{k}}^- \rangle = M_{l\beta}(E, \mathbf{k}), \quad (7)$$

where  $\{E_l\}$  are the discrete energy levels that lie within the continuous range of interest and  $\underline{M}$  is the matrix that couples bound and continuum states. Note that Eqs. (5) and (6) imply that two submatrices, belonging, respectively, to one set of discrete states and to another of continuum states, have been separately diagonalized in a previous step. The resulting eigenfunctions  $\{\Phi_j\}$  and  $\{\chi_{\beta, \mathbf{k}}\}$  represent states that are, respectively, bound and unbound as regards the electronic motion, while they correspond to specific vibrational levels as to the nuclear motion.

The expansion coefficients in Eq. (3) can be determined from the requirement

$$\langle \Phi_l | \hat{H} - E | \Psi_{\text{ap}}^- \rangle = \langle \chi_{\gamma\tau}^- | \hat{H} - E | \Psi_{\text{ap}}^- \rangle = 0, \quad \forall l, \gamma, \tau \quad (8)$$

and the solution of the following set of equations:

$$(E_l - E) a_{l\alpha}(\mathbf{p}) + \sum_{\beta=1}^{m_c} \int \frac{d\mathbf{k}}{(2\pi)^3} M_{l\beta}(E, \mathbf{k}) b_{\beta\alpha}(\mathbf{k}, \mathbf{p}) = 0, \quad (9a)$$

$$\sum_j^{m_d} M_{\gamma j}^{\dagger}(\tau, E) a_{j\alpha}(\mathbf{p}) + \left[ E_{\gamma} + \frac{\tau^2}{2} - E \right] b_{\gamma\alpha}(\tau, \mathbf{p}) = 0, \quad (9b)$$

where  $M_{\gamma j}^{\dagger} = M_{j\gamma}^*$ . Following Fano's approach we remove the singularity at  $E = E_{\gamma} + \frac{1}{2}\tau^2$  in Eq. (9b) by means of coefficients that allow one to satisfy the ingoing wave boundary condition:

$$b_{\gamma\alpha}(\tau, \mathbf{p}) = \lim_{\nu \rightarrow 0} \frac{\sum_{j=1}^{m_d} M_{\gamma j}^{\dagger}(\tau, E) a_{j\alpha}(\mathbf{p})}{E - E_{\gamma} - \frac{\tau^2}{2} - i\nu} + \delta_{\gamma\beta} (2\pi)^3 \delta(\tau - \mathbf{p}). \quad (10)$$

By inserting Eq. (10) into Eq. (9a) and taking into account the following identity, which is valid for every holomorphic function  $f(\mathbf{k})$ :

$$\begin{aligned} \lim_{\nu \rightarrow 0} \int \frac{d\mathbf{k}}{(2\pi)^3} \frac{f(\mathbf{k})}{E - E_{\gamma} - \frac{k^2}{2} - i\nu} \\ = \int \frac{d\mathbf{k}}{(2\pi)^3} \left[ \mathbf{P} \frac{f(\mathbf{k})}{E - E_{\gamma} - \frac{k^2}{2}} \right. \\ \left. + i\pi f(\mathbf{k}) \delta \left[ E - E_{\gamma} - \frac{k^2}{2} \right] \right], \quad (11) \end{aligned}$$

one gets the expression for the coefficients of the discrete states in Eq. (3):

$$a_{j\alpha}(\mathbf{p}) = \sum_{l=1}^{m_d} \Lambda_{jl}^{-1} M_{l\alpha}(E, \mathbf{p}). \quad (12)$$

Note that in (11)  $\mathbf{P}$  indicates the principal part of the integral over  $[E - E_{\gamma} - (k^2/2)]^{-1}$ , while  $\underline{\Lambda}^{-1}$  in (12) is the inverse of the following matrix:

$$\Lambda_{lj} = (E - E_l) \delta_{lj} - \Delta_{lj} - i \frac{\Gamma_{lj}}{2}, \quad (13)$$

with

$$\Delta_{lj} = \sum_{\beta=1}^{m_c} \mathbf{P} \int \frac{d\mathbf{k}}{(2\pi)^3} \frac{M_{l\beta}(E, \mathbf{k}) M_{\beta j}^{\dagger}(\mathbf{k}, E)}{E - E_{\beta} - \frac{k^2}{2}} \quad (14)$$

and

$$\begin{aligned} \Gamma_{lj} = 2\pi \sum_{\beta=1}^{m_c} \int \frac{d\mathbf{k}}{(2\pi)^3} M_{l\beta}(E, \mathbf{k}) M_{\beta j}^{\dagger}(\mathbf{k}, E) \\ \times \delta \left[ E - E_{\beta} - \frac{k^2}{2} \right]. \quad (15) \end{aligned}$$

From Eqs. (14) and (15) one can easily prove that  $\underline{\Delta}$  and  $\underline{\Gamma}$  are Hermitian matrices and  $\underline{\Gamma}$  is positive definite.

It follows that  $\underline{\Lambda}$  can be inverted, and the total wave function  $\Psi_{\alpha\bar{p}}^-$  unambiguously defined as follows:

$$\Psi_{\alpha\bar{p}}^- = \chi_{\alpha\bar{p}}^- + \sum_{j,l=1}^{m_d} \Phi_j^- \Lambda_{jl}^{-1} M_{l\alpha}(E, \mathbf{p}), \quad (16)$$

where

$$\Phi_j^- = \Phi_j + \sum_{\beta=1}^{m_c} \lim_{\nu \rightarrow \infty} \int \frac{d\mathbf{k}}{(2\pi)^3} \frac{\chi_{\beta\mathbf{k}}^- M_{\beta j}^\dagger(\mathbf{k}, E)}{E - E_\beta - \frac{k^2}{2} - i\nu} \quad (17)$$

represents the state  $|\Phi_j\rangle$  modified by an admixture of continuum states.

We observe that, from the knowledge of  $\Psi_{\alpha\bar{p}}^-$ , one can also construct a representation of the  $N$ -electron state corresponding asymptotically to a channel in which the primary electron is emitted with kinetic energy  $\varepsilon_1 = \frac{1}{2}p_1^2$  and the ionized system is described by  $\Psi_{\alpha,p}^-$ . This representation simply consists of an antisymmetrized product of the type  $\Theta_\alpha(\mathbf{p}, \mathbf{p}_1) = \hat{\mathcal{A}}[\Psi_{\alpha\bar{p}}^- \eta_{\mathbf{p}_1}]$  which ignores post-collisional effects and describes the primary electron by means of a wave function  $\eta_{\mathbf{p}_1}$  obtainable, for example, through the solution of a Lippmann-Schwinger equation with an effective potential, as suggested in Ref. [12].

Since we are interested in the global process, which consists of core photoionization plus Auger decay, we have to consider the interaction between molecule and radiation field. This process can be described in a number of different ways [24,25], which, however, give the same final expression for the transition rate from the ground state  $|0\rangle$  of the neutral molecule to the final state  $\Theta_\alpha(\mathbf{p}, \mathbf{p}_1)$ . This expression can be written as follows:

$$W_{0 \rightarrow \alpha}(\mathbf{p}, \mathbf{p}_1) = \int d\omega \int d\hat{\Omega} \sum_{\lambda} \sigma_{0 \rightarrow \alpha}(\mathbf{p}, \mathbf{p}_1; \omega, \lambda) F_{\lambda}(\omega, \hat{\Omega}), \quad (18)$$

where we have separated the spectral function

$$F_{\lambda}(\omega, \hat{\Omega}) = \frac{\omega^2}{(2\pi)^3 c^2} n_{\lambda}(\omega, \hat{\Omega}) \quad (19)$$

from the cross section  $\sigma_{0 \rightarrow \alpha}$  of the transition process. In Eq. (18)  $F_{\lambda}(\omega, \hat{\Omega})$  represents the flux of photons, i.e., the number ( $n_{\lambda}$ ) of photons per unit time and unit area that have angular frequency  $\omega$ , direction  $\hat{\Omega}$ , and polarization  $\lambda$ . As for the cross section one can use the following expression derived from the first-order perturbation theory:

$$\sigma_{0 \rightarrow \alpha}(\mathbf{p}, \mathbf{p}_1; \omega, \lambda) = \delta \left[ (E_0 + \hbar\omega) - \left[ E_{\alpha} + \frac{p^2 + p_1^2}{2} \right] \right] \left[ \frac{4\pi^2 \omega}{c} \right] \times |\langle 0 | \hat{\mathcal{O}}_{\lambda} | \Theta_{\alpha}(\mathbf{p}, \mathbf{p}_1) \rangle|^2 \quad (20)$$

where  $\hat{\mathcal{O}}_{\lambda} = \hat{\mathbf{e}}_{\lambda} \cdot \sum_j q_j \mathbf{r}_j$  is the component of the dipolar operator in the polarization direction  $\lambda$ .

The knowledge of  $\sigma_{0 \rightarrow \alpha}$  allows one to construct the band profile for the transitions from the ground state to

the vibrational levels pertaining to a specific electronic state  $\alpha$  of the doubly ionized molecule. This can be performed by separating in the wave functions that describe the various channels the vibrational part from the electronic part, as will be shown in the next section. The resulting spectral profile can be expressed as a sum of terms, each of which—obtained by inserting Eqs. (16) and (17) into Eq. (20)—is constituted by the following three different contributions:

$$\begin{aligned} \sigma_{0 \rightarrow \alpha} \propto & |\langle 0 | \hat{\mathcal{O}}_{\lambda} | \chi_{\alpha\bar{p}}^- \eta_{\mathbf{p}_1} \rangle| \\ & + \sum_{\beta=1}^{m_c} \lim_{\nu \rightarrow \infty} \int \frac{d\mathbf{k}}{(2\pi)^3} \frac{\langle 0 | \hat{\mathcal{O}}_{\lambda} | \chi_{\beta\mathbf{k}}^- \eta_{\mathbf{p}_1} \rangle \bar{\Gamma}_{\beta\alpha}(\mathbf{k}, \mathbf{p})}{E - E_{\beta} - \frac{k^2}{2} - i\nu} \\ & + \sum_{j,l=1}^{m_d} \langle 0 | \hat{\mathcal{O}}_{\lambda} | \Phi_j \eta_{\mathbf{p}_1} \rangle \Lambda_{jl}^{-1} \langle \Phi_l | \hat{H} - E | \chi_{\alpha\bar{p}}^- \rangle^2 \\ & \times \delta \left[ (E_0 + \hbar\omega) - \left[ E_{\alpha} + \frac{p^2 + p_1^2}{2} \right] \right], \end{aligned} \quad (21)$$

with

$$\begin{aligned} \bar{\Gamma}_{\beta\alpha}(\mathbf{k}, \mathbf{p}) &= \sum_{j,l=1}^{m_d} M_{\beta j}^\dagger(\mathbf{k}, E) \Lambda_{jl}^{-1} M_{l\alpha}(E, \mathbf{p}) \\ &= \sum_{j,l=1}^{m_d} \langle \chi_{\beta\mathbf{k}}^- | \hat{H} - E | \Phi_j \rangle \Lambda_{jl}^{-1} \langle \Phi_l | \hat{H} - E | \chi_{\alpha\bar{p}}^- \rangle. \end{aligned} \quad (22)$$

The first two terms on the right-hand side of Eq. (21) are due to the direct, double ionization process from the ground state  $|0\rangle$  to the final decay channel  $|\chi_{\alpha\bar{p}}^- \eta_{\mathbf{p}_1}\rangle$ . The third term, instead, gives the resonant contribution, i.e., that due to the decay process via intermediate bound states  $\{|\Phi_j\rangle\}$ .

From the inspection of Eq. (21) one can also see that the first two terms contain matrix elements that connect one bound state (the ground) with continua having two unbound electrons. The third term is characterized instead by matrix elements that connect discrete states with one electron continua. Since one can reasonably predict that

$$|\langle 0 | \hat{\mathcal{O}}_{\lambda} | \Phi_j \eta_{\mathbf{p}_1} \rangle| \gg |\langle 0 | \hat{\mathcal{O}}_{\lambda} | \chi_{\alpha\bar{p}}^- \eta_{\mathbf{p}_1} \rangle|, \quad \forall j, \alpha, \mathbf{p}, \quad (23)$$

Eq. (21) can be approximated using only the third term, i.e.,

$$\begin{aligned} \sigma_{0 \rightarrow \alpha} \propto & \left| \sum_{j,l=1}^{m_d} \langle 0 | \hat{\mathcal{O}}_{\lambda} | \Phi_j \eta_{\mathbf{p}_1} \rangle \Lambda_{jl}^{-1} M_{l\alpha}(E, \mathbf{p}) \right|^2 \\ & \times \delta \left[ (E_0 + \hbar\omega) - \left[ E_{\alpha} + \frac{p^2 + p_1^2}{2} \right] \right] \\ & = \left| \sum_{j,l=1}^{m_d} \langle 0 | \hat{\mathcal{O}}_{\lambda} | \Phi_j \eta_{\mathbf{p}_1} \rangle \Lambda_{jl}^{-1} \langle \Phi_l | \hat{H} - E | \chi_{\alpha\bar{p}}^- \rangle \right|^2 \\ & \times \delta \left[ (E_0 + \hbar\omega) - \left[ E_{\alpha} + \frac{p^2 + p_1^2}{2} \right] \right]. \end{aligned} \quad (24)$$

Equation (24) represents an approximation of Eq. (21) and corresponds to the assumption that each transition from the ground to a specific state of the doubly ionized molecule takes place only via intermediate discrete states. If the sum is performed over those terms that correspond to transitions from the ground to vibrational levels pertaining to the same electronic state, one obtains an expression that corresponds to that given in Eq. (1). A detailed comparison between Eq. (1) and the expression obtained by adding terms of the type given in (24) will be performed in the next section, where the vibrational contributions to the cross section will be made evident. At this stage, however, we point out that the main difference between the two expressions consists of the presence of the out-diagonal elements of the matrix  $\underline{\Lambda}^{-1}$  in Eq. (24). Apparently these elements could be eliminated by diagonalizing  $\underline{\Lambda}^{-1}$  and redefining the intermediate bound states  $\{|\Phi_j\rangle\}$ ; however, we observe that this matrix is non-Hermitian and, therefore, in general, nondiagonalizable. Furthermore, if it is diagonalizable its eigenvectors are nonorthogonal with respect to the Hermitian scalar product. It follows that equations—like Eq. (18) of Ref. [10]—that are based on the use of eigenvectors of a non-Hermitian matrix are nonunivocally defined, or at least require the definition of a different type of scalar product. We conclude that the use of Eq. (1) instead of a sum of terms defined as in Eq. (24) is, in general, equivalent to disregarding interference effects due to the nondiagonal terms of  $\underline{\Lambda}^{-1}$ . Finally, we observe that the cross sections defined in Eqs. (21) and (24) depend on the directions of the emitted electrons and, therefore, if the angular distribution of these electrons is not detected in the experiment, one has to average the cross sections over the directions of emission, a process that can be performed using the procedures explained in Sec. III.

### B. Construction of $\{\Phi_j\}$ and $\{\chi_{\beta\mathbf{k}}\}$ and evaluation of the matrix elements

Let us now describe the procedures to construct  $\{\Phi_j\}$  and  $\{\chi_{\beta\mathbf{k}}\}$ —see Eqs. (3)–(7)—starting from a given set of discrete and continuum functions. We consider here the typical case, i.e., one isolated discrete electronic state (closed channel) supporting a number of vibrational levels and several electronic continua (open channels) with their vibrational levels. The molecular Hamiltonian can be written as follows:

$$\hat{H}^{N-1} = \hat{T}_{\mathbf{R}} + \hat{H}_{\text{el}}^{N-1}, \quad (25)$$

where  $\hat{T}_{\mathbf{R}}$  is the nuclear kinetic-energy operator and  $\hat{H}_{\text{el}}^{N-1}$  is the electronic Hamiltonian in which—following the method proposed in Refs. [12,13]—the potential-energy operator has been substituted by its projection onto a multicenter  $L^2$  basis set.

The molecular wave functions  $\{\Phi_j\}$  chosen to represent the intermediate states are made up as follows:

$$\Phi_j(\mathbf{r}, \mathbf{R}) = \varphi^{\text{el}}(\mathbf{r}, \mathbf{R}) v_j(\mathbf{R}), \quad (26)$$

where the electronic part  $\varphi^{\text{el}}$ —which depends parametrically on the ensemble of the nuclear coordinates ( $\mathbf{R}$ )—is

a linear combination of Slater determinants constructed using one of the standard techniques [Hartree-Fock (HF), many-configuration self-consistent-field (MC-SCF), configuration-interaction (CI)] for bound-state calculations. The vibrational functions  $\{v_j\}$  that classify the intermediate states can be obtained through the solution of the following differential equation:

$$[\hat{T}_{\mathbf{R}} + E_{\varphi}^{\text{el}}(\mathbf{R})]v_j = \mathcal{E}_j v_j, \quad (27)$$

where  $E_{\varphi}^{\text{el}}(\mathbf{R}) = (\varphi^{\text{el}} | \hat{H}_{\text{el}}^{N-1} | \varphi^{\text{el}})$  is the electronic potential-energy surface relative to the intermediate bound state. Note that to improve the representation one can also take into account the matrix element  $(\varphi | \hat{T}_{\mathbf{R}} | \varphi)$ , which, in the case of an isolated electronic state, simply introduces a local correction to  $E_{\varphi}^{\text{el}}(\mathbf{R})$ . In the most general case, when several discrete electronic states are present, one can proceed either in the context of the BO approximation, i.e., treating each channel separately, or through the inclusion of the couplings due to the nuclear motion and the diagonalization of  $H^{N-1}$  in the subspace of the intermediate discrete states. This second alternative is usually required only if the electronic states are not well separated in energy.

Regarding the open channels, we adopt the procedure of Ref. [13] and construct a set of functions made up as follows:

$$\chi_{\alpha\mathbf{k}}(\mathbf{r}, \mathbf{R}) = \chi_{\alpha\mathbf{k}}^{\text{el}}(\mathbf{r}, \mathbf{R}) \theta_{n_{\alpha}}^{\alpha}(\mathbf{R}), \quad (28)$$

$$\chi_{\alpha\mathbf{k}}^{\text{el}}(\mathbf{r}, \mathbf{R}) = \hat{\mathcal{A}}[\eta_{\mathbf{k}}(\mathbf{r}_1, \mathbf{R}) \sigma(s_1) \Theta_{\alpha}(2, \dots, N-1; \mathbf{R})], \quad (29)$$

$$[\hat{T}_{\mathbf{R}} + E_{\alpha}^{\text{el}}(\mathbf{R})] \theta_{n_{\alpha}}^{\alpha} = \mathcal{E}_{n_{\alpha}}^{\alpha} \theta_{n_{\alpha}}^{\alpha}, \quad (30)$$

where  $\hat{\mathcal{A}}$  is the antisymmetrizer that includes also the normalization constant,  $\sigma$  is the spin function, and the following relationships are satisfied:

$$(\Theta_{\beta} | \hat{H}_{\text{el}}^{N-2} | \Theta_{\alpha}) = E_{\alpha}^{\text{el}}(\mathbf{R}) \delta_{\alpha\beta}, \quad (31)$$

$$(\eta_{\mathbf{k}}(\mathbf{r}_j) | \Theta_{\alpha}(1, \dots, N-2))_j = 0, \quad \forall \alpha, j, \mathbf{k}, \quad (32)$$

$$(\eta_{\mathbf{k}} | \eta_{\mathbf{p}}) = (2\pi)^3 \delta(\mathbf{k} - \mathbf{p}). \quad (33)$$

In Eqs. (31)–(33)  $(|)$  indicates the integration over the electronic coordinates; furthermore, the wave functions  $\{\Theta_{\alpha}\}$ , which represent discrete electronic states of the doubly ionized molecules, are linear combinations of Slater determinants made up, in our procedure, by orthogonal orbitals that are eigenfunctions of the same effective Hartree-Fock operator. The number and type of determinants used for the expansion of  $\Theta_{\alpha}$  depend on the required accuracy of the calculation. The continuum orbital  $\eta_{\mathbf{k}}$ , which is orthogonal to the space of the bound orbitals, is obtained by solving a Lippmann-Schwinger equation as suggested in Refs. [12,13].

Using Eqs. (28)–(30) and neglecting the effects of the nuclear kinetic-energy operator on the electronic wave functions, one obtains the following expression for the matrix elements that couple the continuum functions:

$$\begin{aligned} & \langle \chi_{\beta k} | \hat{H}^{N-1} - E | \chi_{\alpha p} \rangle \\ & \simeq \langle \theta_{n_\beta}^\beta | (\chi_{\beta k}^{\text{el}} | \mathcal{E}_{n_\alpha}^\alpha - E_\alpha^{\text{el}}(\mathbf{R}) + \hat{H}_{\text{el}}^{N-1} - E | \chi_{\alpha p}^{\text{el}}) | \theta_{n_\alpha}^\alpha \rangle . \end{aligned} \quad (34)$$

In Ref. [13] we have proposed a procedure for obtaining eigenfunctions  $\{\chi_{\alpha p}^{\text{el}-}\}$ , which present the correct asymptotic behavior and diagonalize the electronic matrix  $(\chi_{\beta k}^{\text{el}} | \hat{H}_{\text{el}}^{N-1} - E | \chi_{\alpha p}^{\text{el}})$  to give

$$\begin{aligned} (\chi_{\beta k}^{\text{el}-} | \hat{H}_{\text{el}}^{N-1} - E | \chi_{\alpha p}^{\text{el}-}) &= [E_\alpha^{\text{el}}(\mathbf{R}) + \frac{1}{2}p^2 - E] \\ & \times \delta_{\alpha\beta}(2\pi)^3 \delta(\mathbf{k} - \mathbf{p}) . \end{aligned} \quad (35)$$

Using these functions instead of the  $\{\chi_{\alpha k}^{\text{el}}\}$  in Eq. (28) we obtain a set of wave functions

$$\chi_{\alpha k}^-(\mathbf{r}, \mathbf{R}) = \chi_{\alpha k}^{\text{el}-}(\mathbf{r}, \mathbf{R}) \theta_{n_\alpha}^\alpha(\mathbf{R}) , \quad (36)$$

which diagonalize the molecular Hamiltonian in the BO approximation

$$\begin{aligned} \langle \chi_{\beta k}^- | \hat{H}^{N-1} - E | \chi_{\alpha p}^- \rangle &= (\mathcal{E}_{n_\alpha}^\alpha + \frac{1}{2}p^2 - E) \delta_{\alpha\beta}(2\pi)^3 \\ & \times \delta(\mathbf{k} - \mathbf{p}) \delta_{n_\alpha n_\beta} \end{aligned} \quad (37)$$

and present the correct asymptotic behavior. We observe that the use of the BO approximation is less justified when the electronic levels of the doubly ionized molecule are close in energy. In these cases, the quality of the representation can be improved by including in the procedures of Ref. [13] the couplings among electronic functions that are due to the nuclear kinetic-energy operator.

After the construction of the two subsets of discrete and continuum functions one has simply to evaluate their coupling matrix elements  $\{M_{l\beta}(E, \mathbf{k})\}$  in order to obtain the eigenfunction  $\Psi_{\alpha p}^-$  of  $\hat{H}^{N-1}$  at the energy  $E = \mathcal{E}_{n_\alpha}^\alpha + \frac{1}{2}p^2$ . From Eq. (7) and making use of the BO

approximation one gets

$$\begin{aligned} M_{l\beta}(E, \mathbf{k}) &= \langle \Phi_l | \hat{H}^{N-1} - E | \chi_{\beta k}^- \rangle \\ & \simeq \langle v_l | (\varphi^{\text{el}} | \mathcal{E}_{n_\beta}^\beta - E_\beta^{\text{el}}(\mathbf{R}) \\ & \quad + \hat{H}_{\text{el}}^{N-1} - E | \chi_{\beta k}^{\text{el}-}) | \theta_{n_\beta}^\beta \rangle \\ & = \langle v_l | M_\beta^{\text{el}}(E, \mathbf{k}; \mathbf{R}) | \theta_{n_\beta}^\beta \rangle , \end{aligned} \quad (38)$$

where  $M_\beta^{\text{el}}$ , implicitly defined through Eq. (38), represents the electronic coupling between the discrete state and the continuum state ( $\beta$ ). For calculating the spectral parameters  $\{\Gamma_{l\beta}\}$  and  $\{\Delta_{l\beta}\}$  from the knowledge of  $\{M_\beta^{\text{el}}\}$  one has simply to apply the previous definitions. In particular, using the following resolution of the identity:  $\hat{I} = \sum_{n_\beta} |\theta_{n_\beta}^\beta\rangle \langle \theta_{n_\beta}^\beta|$ , given in terms of the vibrational functions of the electronic state  $\beta$ , one gets from Eq. (15)

$$\Gamma_{l\beta} = \langle v_l | \Gamma^{\text{el}}(E; \mathbf{R}) | v_j \rangle , \quad (39)$$

where

$$\begin{aligned} \Gamma^{\text{el}}(E; \mathbf{R}) &= 2\pi \sum_{\beta=1}^{m_c} \int \frac{d\mathbf{k}}{(2\pi)^3} M_\beta^{\text{el}}(E, \mathbf{k}; \mathbf{R}) M_\beta^{\text{el}\dagger}(\mathbf{R}; \mathbf{k}, E) \\ & \times \delta \left[ E - \mathcal{E}_{n_\beta}^\beta - \frac{k^2}{2} \right] . \end{aligned} \quad (40)$$

The integrals in Eq. (40) can be calculated analytically using the procedures explained in Refs. [26,27], and this fact allows one to obtain an efficient and accurate evaluation of  $\Gamma_{l\beta}$ .

A similar approach can be used also for  $\Delta_{l\beta}$ . However, in this case, an approximation has to be introduced in order to perform analytically the integration over  $\mathbf{k}$  in Eq. (14), that is,

$$\begin{aligned} \Delta_{l\beta} &= \sum_{\beta=1}^{m_c} \sum_{n_\beta} P \int \frac{d\mathbf{k}}{(2\pi)^3} \frac{\langle v_l | M_\beta^{\text{el}}(E, \mathbf{k}; \mathbf{R}) | \theta_{n_\beta}^\beta \rangle \langle \theta_{n_\beta}^\beta | M_\beta^{\text{el}\dagger}(\mathbf{R}; \mathbf{k}, E) | v_j \rangle}{E - \mathcal{E}_{n_\beta}^\beta - \frac{k^2}{2}} \\ & \simeq \left\langle v_l \left| \sum_{\beta=1}^{m_c} P \int \frac{d\mathbf{k}}{(2\pi)^3} \frac{M_\beta^{\text{el}}(E, \mathbf{k}; \mathbf{R}) M_\beta^{\text{el}\dagger}(\mathbf{R}; \mathbf{k}, E)}{E - E_\beta(\mathbf{R}) - \frac{k^2}{2}} \right| v_j \right\rangle \\ & = \langle v_l | \Delta^{\text{el}}(E; \mathbf{R}) | v_j \rangle . \end{aligned} \quad (41)$$

Such an approximation is equivalent to neglecting the kinetic energy of the nuclei with respect to their potential energy at each internuclear distance, a fact that allows one to use the analytical procedures of Refs. [26,27] for the evaluation of  $\Delta^{\text{el}}(E, \mathbf{R})$ .

From the knowledge of  $\{\Gamma_{l\beta}\}$  and  $\{\Delta_{l\beta}\}$  and of the vibrational functions defined in Eqs. (26) and (36) one can use Eq. (24) to calculate the band profile for the transitions from the ground to the vibrational levels of the elec-

tronic state  $|\chi_{\alpha k}^{\text{el}-}\rangle$ . The resulting equation is

$$\begin{aligned} \sigma_{|0\rangle \rightarrow |\chi_{\alpha k}^{\text{el}-}\rangle} &\propto \sum_{n_\alpha} \left| \sum_{j,l=1}^{m_b} \langle v_j | \hat{V}' | v_l \rangle \Lambda_{jl}^{-1} \langle v_l | \hat{V} | \theta_{n_\alpha}^\alpha \rangle \right|^2 \\ & \times \delta \left[ (E_0 + \hbar\omega) - \left[ \mathcal{E}_{n_\alpha}^\alpha + \frac{p^2 + p_1^2}{2} \right] \right] , \end{aligned} \quad (42)$$

where

$$\hat{V}' = (\varphi_g^{\text{el}} | \hat{O}_\lambda | \varphi^{\text{el}} \eta_{p1}), \quad \hat{V} = M_\alpha^{\text{el}}(E, \mathbf{p}; \mathbf{R}), \quad (43)$$

and the ground state in its lowest vibrational state is represented by

$$\Phi_g(\mathbf{r}, \mathbf{R}) = \varphi_g^{\text{el}}(\mathbf{r}, \mathbf{R}) v_g^{\text{vib}}(\mathbf{R}). \quad (44)$$

Equation (42) is the correct generalization of Eq. (1), since it takes into account the interference effects due to the out-diagonal elements of the matrix  $\underline{\Lambda}^{-1}$  and does not introduce any problems related to the diagonalization of non-Hermitian matrices. If one is interested in also evaluating the contributions to the cross section due to the direct double ionization process, one should start from Eq. (21) instead of Eq. (24) while keeping the other procedures exactly the same.

### III. THE AUGER SPECTRA OF CARBON MONOXIDE

Using the procedures explained in Sec. II B we have reproduced the Auger spectra of the CO molecule ionized in its deepest shells, i.e., in the  $1s$  core orbital of the oxygen and carbon atoms. Our attention has been focused on the vibrational analysis of the Auger bands that we have calculated *ab initio* over the entire energy range of interest and compared with the experimental spectra recorded by Moddeman *et al.* [19]. Interesting regions of these spectra have been analyzed in more detail, like that between 249 and 257 eV in the carbon spectrum where the very narrow  $B^1\Sigma^+$  band and those originating from the superposition of the vibrational progressions of  $A^1\Pi$  and  $X^1\Sigma^+$  are located. These two bands have also been considered in the oxygen spectrum and the corresponding region between 497 and 506 eV has been analyzed in detail. The results obtained from the application of our method have been compared with the high-resolution spectra recorded by Correia *et al.* [9].

The calculations described in the present paper have been carried out using a basis set [28] of  $[9s/5p]$  modified Gaussian functions [29] contracted to  $[4s/2p]$  on each atomic center. This basis set has been extended through the inclusion of four  $s$ -,  $p$ -, and  $d$ -type functions both on the carbon atom with orbital exponents ( $\alpha$ ) respectively given by ( $\alpha_s = 1.9\text{-}0.95\text{-}0.1011\text{-}0.0449$ ,  $\alpha_p = 6.5\text{-}3.0\text{-}1.85\text{-}0.0721$ ,  $\alpha_d = 3.978\text{-}1.7145\text{-}1.17\text{-}0.772$ ) and on the oxygen atom ( $\alpha_s = 1.2\text{-}0.60\text{-}0.2614\text{-}0.1334$ ,  $\alpha_p = 7.0\text{-}3.8\text{-}1.80\text{-}0.1179$ ,  $\alpha_d = 3.838\text{-}1.717\text{-}1.212\text{-}0.808$ ). The exponents of these functions have been optimized following the procedures of Ref. [12]. The electronic wave functions at each internuclear distance have been calculated using a two-step process: (a) SCF optimization of the molecular orbitals; (b) a CI calculation performed including all the single and double excitations in a given active space.

As for the ground state, we have optimized first in a self-consistent way the occupied and first virtual orbitals of the  $\sigma$  and  $\pi$  symmetries. Secondly, we have constructed the correlated wave function through the diagonalization of the Hamiltonian matrix in the space of the electronic configurations that can be obtained using

( $3\sigma, \dots, 6\sigma, 1\pi, 2\pi$ ) as active orbitals and considering all the possible single and double excitations in this space.

As for the two resonant Auger states, we have performed first separate restricted Hartree-Fock calculations for the two doublet states having, respectively, the  $1\sigma$  and  $2\sigma$  orbitals half-occupied and then optimized the first virtual orbital of the  $\sigma$  and  $\pi$  symmetries. Secondly, we have constructed the correlated wave functions by diagonalizing the Hamiltonian matrix in the space of the configurations that can be obtained using ( $5\sigma, 6\sigma, 1\pi, 2\pi$ ) as active orbitals and considering all the possible single and double excitations in this space (while keeping the  $1\sigma$  or  $2\sigma$  orbital half-filled).

Finally, the electronic states of the doubly ionized target have been represented using a set of molecular orbitals obtained as eigenfunctions of the following Fock-type operator:  $\hat{F} = \hat{h} + \sum_j a_j (2\hat{J}_j - \hat{K}_j)$ , where  $a_j$  is the average occupation number of the orbital  $j$  obtained from the average of its occupation numbers in the final dicationic states. The correlated wave functions derive from the diagonalization of the Hamiltonian matrix in the space of the electronic configurations that can be constructed by considering all the possible single and double excitations in the space of the ( $3\sigma, 4\sigma, 5\sigma, 6\sigma, 1\pi, 2\pi$ ) orbitals.

It is well known that in this type of problem the use of correlated wave functions is essential, since one needs to have the correct ordering of the states and sufficiently accurate potential-energy curves and matrix elements in the relevant regions. This is particularly true for the three lowest singlet states ( $X^1\Sigma^+$ ,  $A^1\Pi$ ,  $B^1\Sigma^+$ ) of the doubly ionized molecule, the curves of which present a complicated behavior between 1.5 and 3 a.u. that is due to avoided crossings of the two  $^1\Sigma^+$  states, crossing of  $X^1\Sigma^+$  and  $A^1\Pi$  in the vicinity of the neutral ground-state equilibrium distance, crossing of  $B^1\Sigma^+$  and  $A^1\Pi$  at shorter distance, and the presence of two minima in the curve of  $B^1\Sigma^+$ . The behavior of these curves—already discussed in previous papers [9,11,23]—is correctly reproduced by our correlated wave functions, as shown in Fig. 1. We observe that, even if the energies calculated in these papers are higher than those obtained in Ref. [23] through a more sophisticated CI calculation, the form of our curves and the values obtained for the corresponding spectroscopic constants—see Table I—agree very well

TABLE I. The first three singlet states of  $\text{CO}^{2+}$ : equilibrium positions ( $R_{\text{eq}}$ ) in Å, vibrational frequencies ( $\omega_e$ ) in  $\text{cm}^{-1}$ , and vertical excitation energies ( $T_e$ ) in eV, these last calculated with respect to the energy of the lowest ( $^3\Pi$ ) electronic state of  $\text{CO}^{2+}$  at its equilibrium position ( $R = 1.261$  Å). The results of this work are reported in the first row of each entry, while those of Ref. [23] are given in the second row.

Quantity	$X^1\Sigma^+$	$B^1\Sigma^+$	$A^1\Pi$
$R_{\text{eq}}$	1.171	1.090	1.257
	1.170	1.097	1.264
$\omega_e$	1959	2440	1546
	1899	2492	1449
$T_e$	0.27	4.51	0.38
	0.25	4.37	0.52

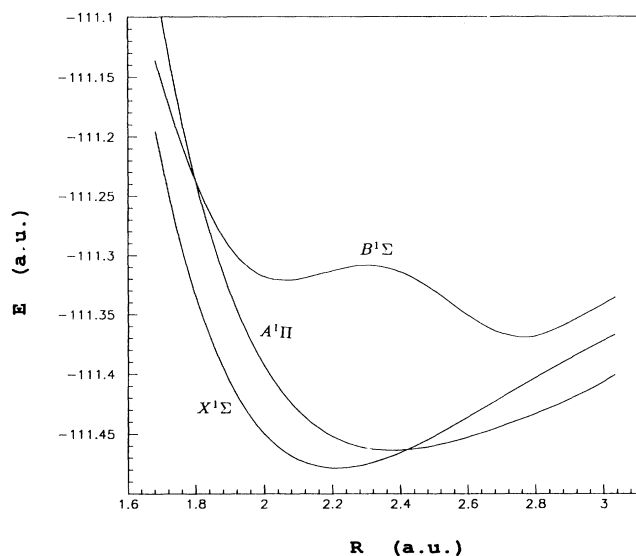


FIG. 1. Behavior with the internuclear distance of the energy curves of the first three singlet states of the doubly ionized molecule. All the quantities are given in a.u.

with those reported in Ref. [23].

Since in this type of problem the role of the spectral parameters is decisive, we present in Fig. 2 for the same three electronic states the behavior with the internuclear distance of the square modulus of the electronic matrix elements  $\{M_{\beta}^{el}\}$ —see Eq. (38)—averaged over the directions ( $\mathbf{k}$ ) of the Auger electron. We see that these matrix elements vary quite rapidly with the internuclear distance because of the changes in the structure of the wave functions, and therefore the “constant resonance width” ap-

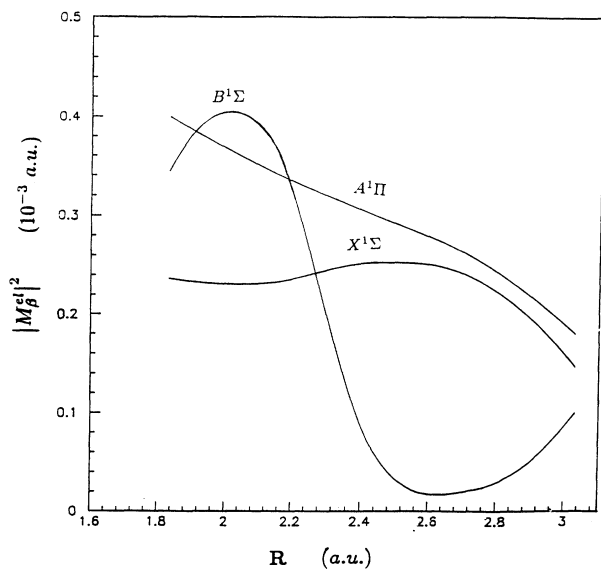


FIG. 2. Behavior with the internuclear distance of the square modulus of the matrix elements—defined in Eq. (38) and averaged over the directions of the Auger electron—for the first three singlet states of the doubly ionized molecule. All the quantities are given in a.u.

proximation, used in previous calculations [9,11], is not appropriate in this case.

Finally, we observe that, even if our wave functions are correlated enough to produce energy curves of the proper form and with the correct ordering at each internuclear distance, errors can be introduced when energy differences are considered. These errors, which can be even of the order of 1–2 eV, are due to the unbalanced introduction of the correlation effects in the representation of different states. On the other hand, a certain degree of uncertainty is also present in the experimental determination of the kinetic energy of the Auger electrons, as one can see, for example, by comparing the carbon Auger spectrum recorded in the region between 249 and 257 eV by Moddeman *et al.* [19] with that recorded by Correia *et al.* [9]. To correct this deficiency in the simplest way without increasing the computational effort we have used two parameters. One is a global shift of the energies performed in such a way as to center the exact position of a specific band in the spectrum of interest. The other is an energy scale factor that corrects the progressive worsening of the state representation when the degree of excitation is increased. The use of these two simple parameters—applied to energy values that are already close to the exact ones—allows us to obtain a very satisfactory correspondence between experimental and calculated energies and therefore to compare in a consistent way experimental and “theoretical” Auger spectra.

As regards the construction of the vibrational eigenfunctions, we have solved the problem by expanding each of them in terms of a basis set of Gaussian functions. In our procedure the electronic curves have been interpolated by means of polynomials of various degree, and several Gaussian functions have been centered at equally spaced positions along each curve in order to represent the vibrational functions. This type of approach allows us to reduce the problem of solving the differential equations defined in Eqs. (27) and (30) to that of diagonalizing matrices, the elements of which are integrals that can be performed analytically because of the representation chosen for the potential. The stability of the solutions obtained in this way has been checked by increasing the degree of the polynomials used for the interpolations and the number of Gaussians used for the expansions.

Let us now construct the “theoretical” carbon and oxygen Auger spectra. As already explained in the previous sections, we reproduce the experimental spectrum by superposing contributions of the type given in Eq. (18), each one corresponding to the decay rate of a specific process. We assume that the molecule interacts with a monochromatic, linearly polarized radiation, and therefore we put in Eq. (19)  $n_{\lambda} = n_0 \delta(\omega - \omega_0) \delta(\hat{\Omega} - \hat{\Omega}_0) \delta_{\lambda, \lambda_0}$ . Furthermore, since each molecule is randomly oriented in the space, we use in Eq. (18) a cross section that is the average of those obtained by choosing  $\lambda$ , in Eq. (20), equal, respectively, to  $\hat{x}$ ,  $\hat{y}$ , and  $\hat{z}$ , i.e., by averaging the three cross sections relative to the three dipole components.

Finally, we observe that in the experiments of interest the Auger electrons are collected by recording only their

kinetic energy ( $\epsilon = p^2/2$ ) and not the direction of emission and that, furthermore, no information is given on the primary electrons. It follows that, to reproduce the experimental profiles starting from the cross section defined in Eq. (42), one has to average over the directions  $\hat{p}$  of the Auger electron and to integrate over the momentum  $\mathbf{p}_1$  of the primary electron. The resulting expression is, thereby, the following

$$\bar{\sigma}_{0 \rightarrow \alpha}(\omega_0; \epsilon) \propto \frac{1}{3} \sum_{\lambda_0}^{(\hat{x}, \hat{y}, \hat{z})} \int d\hat{p} \int d\mathbf{p}_1 \sigma_{|0\rangle \rightarrow |\chi_{\alpha}^{el-}\rangle}(\mathbf{p}, \mathbf{p}_1; \omega_0, \lambda_0), \quad (45)$$

where the integration over  $\mathbf{p}_1$  is really performed only over the directions of  $\mathbf{p}_1$ , since its modulus is fixed at  $p_1(\epsilon) = \{2[(E_0 + \hbar\omega) - (\mathcal{E}_{n_{\alpha}}^{\alpha} + \epsilon)]\}^{1/2}$  by the  $\delta$  function in Eq. (42). Note that using the procedures explained in Refs. [26,27] one can evaluate Eq. (45) directly and without repeating the calculations of  $\sigma_{|0\rangle \rightarrow |\chi_{\alpha}^{el-}\rangle}(\mathbf{p}, \mathbf{p}_1; \omega_0, \lambda_0)$  at various directions of  $\mathbf{p}$  and  $\mathbf{p}_1$ . The final expression used for reproducing the whole experimental spectrum is, therefore, the following:

$$I(\omega_0; \epsilon) \propto \sum_{\alpha} \bar{\sigma}_{0 \rightarrow \alpha}(\omega_0; \epsilon), \quad (46)$$

where the sum is over the final electronic states of the doubly ionized molecule and the intensity is given as a function of the energy of the Auger electron.

Note that the "theoretical" spectrum  $I(\omega_0; \epsilon)$ , defined in Eq. (46), is proportional to the sum of the cross sections, since the absolute intensities of the lines depend on the characteristics of the specific experiment. Finally, it should be remembered that the finite-resolution power of the spectrometer introduces an "instrumental" width that adds up to the intrinsic width of the lines. In order to take into account this effect, we make a convolution of the cross sections in Eq. (46) with a normalized Gaussian function having a width that is inversely proportional to the experimental resolution. The resulting formula for the experimental spectrum is thus given by

$$I_{\text{expt}}(\omega_0; \epsilon) \propto \sum_{\alpha} \frac{1}{\gamma \sqrt{\pi}} \int_{-\infty}^{\infty} \bar{\sigma}_{0 \rightarrow \alpha}(\omega_0; \tau) e^{-(\tau - \epsilon)^2 / \gamma^2} d\tau, \quad (47)$$

where  $\gamma$  is an empirical parameter that depends on the specific experiment.

In this paper we have used for  $I_{\text{expt}}$  the cross-section expression given in Eq. (42); this means that we have disregarded the contributions to the spectral profile that are due to the direct double ionization processes and appear in the more general definition of the cross section given in Eq. (21). Furthermore, we have applied the procedures explained in Sec. II B, thereby assuming the validity of the BO approximation and Eq. (41). The quality of these approximations can be judged by looking at the results obtained from our calculations.

Let us consider first the carbon *K-LL* Auger spectrum. In order to make the relative importance of the electron-

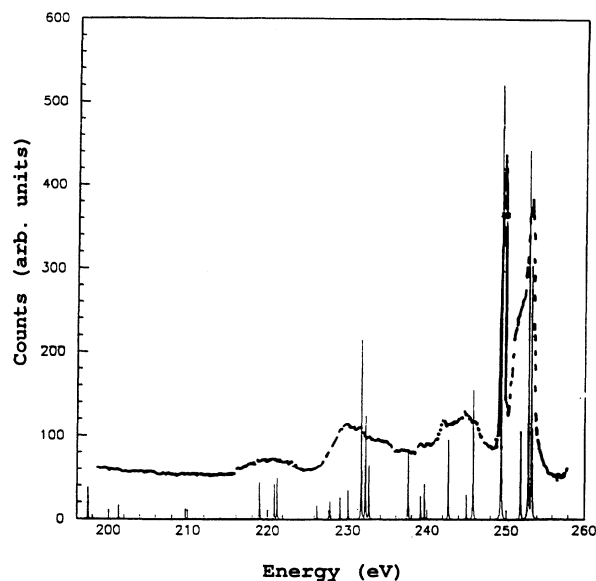


FIG. 3. Carbon Auger spectrum (lower) obtained by considering only the electronic decay processes and compared with the experimental spectrum (upper). In abscissas the kinetic energies of the Auger electron are given in eV, while in ordinates the spectral intensities are in arbitrary units.

ic, vibrational, and instrumental effects evident, we have produced three spectra, shown, respectively, in Figs. 3–5. In the first we have considered only the electronic transitions. This is equivalent to assuming that these processes are much faster than the nuclear motion and, therefore, that the vibrational effects are negligible. For calculating this spectrum, the molecule has been frozen at its

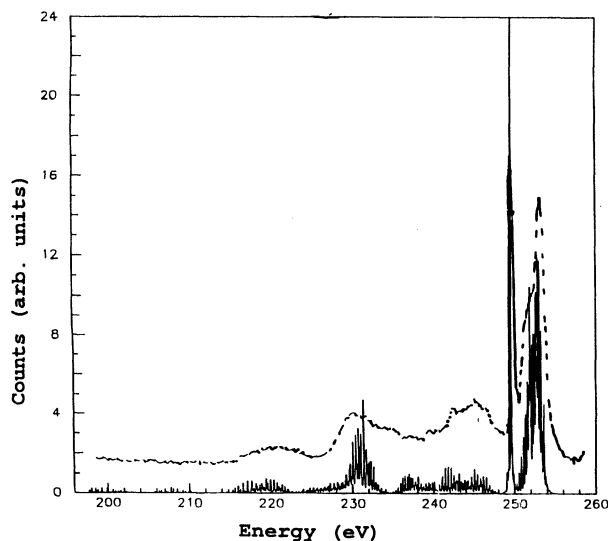


FIG. 4. Carbon Auger spectrum (lower) obtained by considering the vibrational transitions and compared with the experimental spectrum (upper). In abscissas the kinetic energies of the Auger electron are given in eV, while in ordinates the spectral intensities are in arbitrary units.

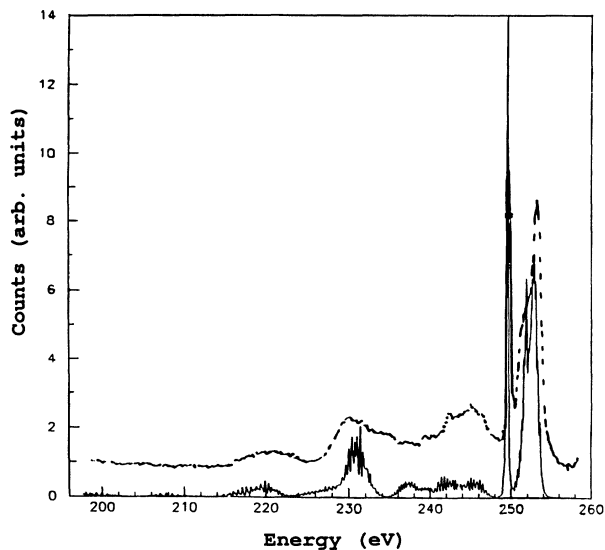


FIG. 5. Carbon Auger spectrum (lower) obtained by considering the vibrational transitions plus the instrumental broadening and compared with the experimental spectrum (upper). In abscissas the kinetic energies of the Auger electron are given in eV, while in ordinates the spectral intensities are in arbitrary units.

ground-state equilibrium geometry and only transitions to final electronic states through the isolated electronic resonance have been taken into account.

The resulting spectrum, compared in Fig. 3 with the experimental one, shows that the electronic transitions are, in general, shifted with respect to the maximum of the corresponding experimental bands, a fact that confirms the presence of important vibrational effects. Furthermore, one can observe that the number of relevant electronic transitions is much larger than that (18) allowed by the independent-particle model, a fact that indicates the importance of the correlation effects. From this comparison one can conclude that a purely electronic spectrum gives only a rough representation of the experimental one and, in particular, that it does not allow one to reproduce the specific features of the spectrum, e.g., in this case, the isolated, very narrow band around 250 eV.

When the vibrational effects are taken into account, i.e., all the transitions that connect intermediate and final vibrational levels are included in the calculations, one obtains a quantitative agreement between theory and experiment over the entire energy range of interest—see Fig. 4. This agreement becomes even more striking—see Fig. 5—when the instrumental broadening is included in the calculations through the use of Eq. (47) with  $\gamma=0.1$  eV.

In order to test the ability of our method to predict the details of a particular spectral region, we have reproduced the band profiles in the region between 249 and 257 eV where the vibrational progressions pertaining to the first three singlet states of the doubly ionized molecule are located and accurate experimental data are available—see Ref. [9]. A comparison between the results obtained using Eq. (47) and the experimental

spectrum—see Fig. 6—confirms that this method represents an efficient tool for also analyzing the fine-structure details in a small spectral region. Furthermore, a careful analysis of the results obtained from our calculations shows that the vibrational levels of the  $B^1\Sigma^+$  state that give rise to transitions of appreciable intensity are only three, much fewer than in the case of the other electronic states. Among these three levels, the intensity of the second one is greater, in an order of magnitude, than those of the other two levels. These facts—which are due to the predissociative character of the  $B^1\Sigma^+$  curve having its first minimum near to that of the carbon Auger state  $C(1s^{-1})$ —produce the isolated, very narrow band characteristic of the spectrum.

The same type of analysis also has been performed on the oxygen  $K$ - $LL$  Auger spectrum. In Fig. 7 we compare the electronic spectrum with the experimental one and observe that, also in this case, there is no simple correspondence between electronic transitions and spectral profile because of the presence of other important effects. Furthermore, the number and relative intensities of the various transitions are quite different as compared with those in the carbon Auger spectrum, a fact that can be ascribed to the different nature of the intermediate electronic states. By taking into account both vibrational transitions and instrumental broadening, this last through Eq. (47) with  $\gamma=0.2$  eV, we have produced two spectra—shown, respectively, in Figs. 8 and 9—which compare very satisfactorily with the experimental one. The only appreciable difference with respect to the experimental data is found in the region between 482 and 489 eV, where the relative intensity of the first band is lower than that of the second one, a result obtained also by

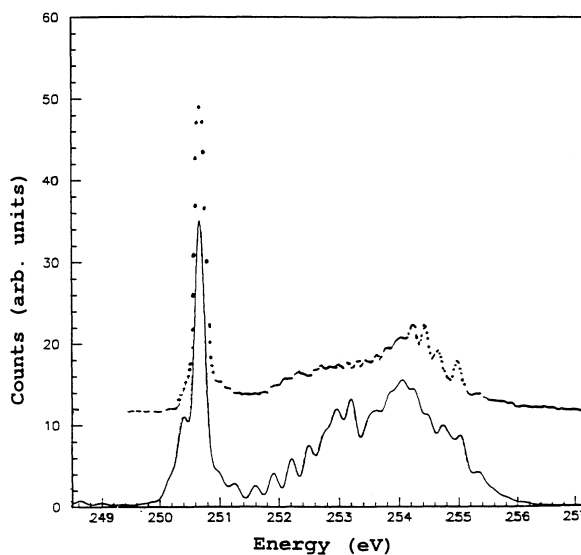


FIG. 6. Selected band profiles in the carbon Auger spectrum (lower) obtained considering vibrational transitions plus instrumental broadening and compared with the experimental spectrum (upper). In abscissas the kinetic energies of the Auger electron are given in eV, while in ordinates the spectral intensities are in arbitrary units.

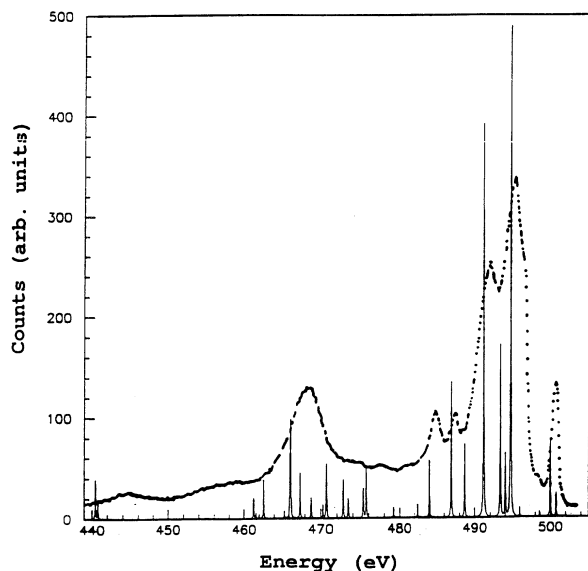


FIG. 7. Oxygen Auger spectrum (lower) obtained by considering only the electronic decay processes and compared with the experimental spectrum (upper). In abscissas the kinetic energies of the Auger electron are given in eV, while in ordinates the spectral intensities are in arbitrary units.

Cederbaum *et al.* Ref. [11].

Finally, we have analyzed in greater detail the spectral region between 497 and 506 eV, which corresponds to that between 249 and 257 eV in the carbon spectrum. Also, in this case the calculated spectral profile, shown in Fig. 10, reproduces very accurately the details of the high-resolution spectrum reported in Ref. [9]. From the

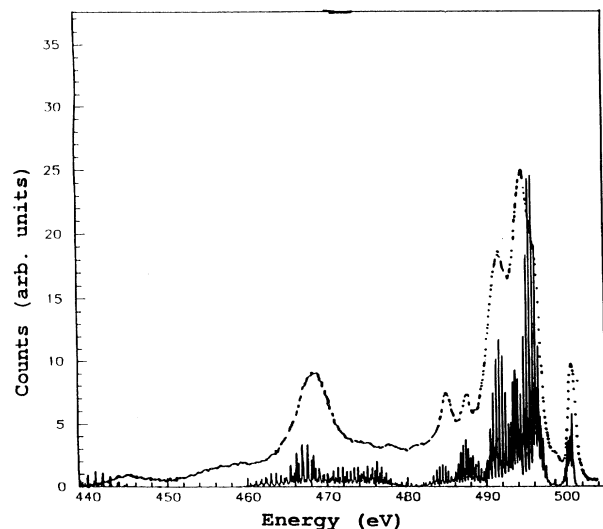


FIG. 8. Oxygen Auger spectrum (lower) obtained by considering the vibrational transitions and compared with the experimental spectrum (upper). In abscissas the kinetic energies of the Auger electron are given in eV, while in ordinates the spectral intensities are in arbitrary units.

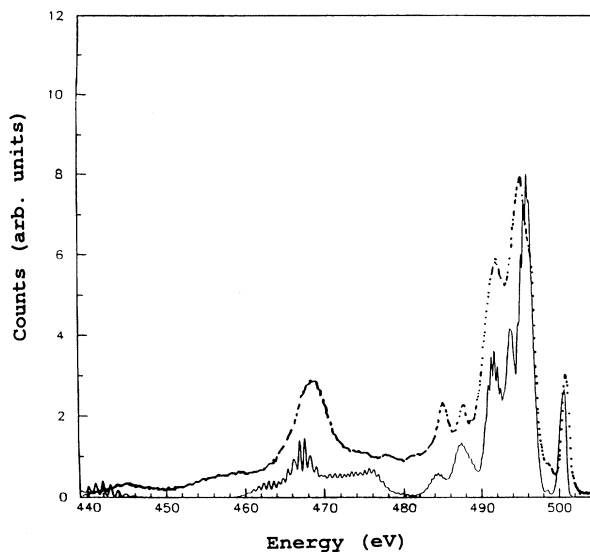


FIG. 9. Oxygen Auger spectrum (lower) obtained by considering the vibrational transitions plus the instrumental broadening and compared with the experimental spectrum (upper). In abscissas the kinetic energies of the Auger electron are given in eV, while in ordinates the spectral intensities are in arbitrary units.

analysis of our data we have also found that the small bump around 498.8 eV is produced by transitions to vibrational levels that are supported by a  $^3\Sigma^+$  electronic state, as suggested in Ref. [11], and not by the  $B^1\Sigma^+$  state, as proposed in Ref. [9]. We conclude this section by pointing out that the comparison between carbon and

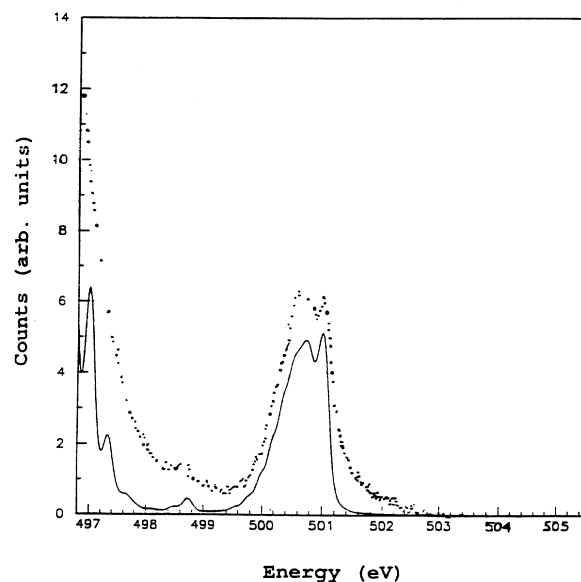


FIG. 10. Selected band profile in the oxygen Auger spectrum (lower) obtained by considering the vibrational transitions plus the instrumental broadening and compared with the experimental data (upper). In abscissas the kinetic energies of the Auger electron are given in eV, while in ordinates the spectral intensities are in arbitrary units.

oxygen spectra confirms that, although the final dicationic states are the same, the profile of the two spectra are completely different, a fact which can be ascribed to the local character both of the intermediate electronic states and of several final states of the doubly ionized molecule.

#### IV. CONCLUSIONS

A general expression for predicting the vibrational profile of a molecular Auger spectrum has been derived. The validity of this expression is not limited by any particular assumption either on the number or the type of resonances or on the internuclear coordinate dependence of the various spectral parameters. In deriving this expression the problems related to the use of non-Hermitian matrices have been explicitly taken into account and

solved unambiguously.

Specific procedures for implementing cross-section calculations in the BO approximation have been proposed and the relationship between the "theoretical" cross section and the experimental spectrum has been discussed. Very satisfactory results have been obtained in reproducing the carbon and oxygen *K-LL* Auger spectra over the whole energy range of interest. Specific spectral regions of small extension have also been reproduced in greater detail.

#### ACKNOWLEDGMENT

This work was partly supported by "Progetto Finalizzato Materiali Speciali per Tecnologie Avanzate del CNR."

- 
- [1] M. Thompson, M. Baker, A. Christie, and J. Tyson, *Auger Electron Spectroscopy* (Wiley, New York, 1985).
- [2] I. Harrison, G. C. King, and L. Avaldi, *J. Phys. B* **21**, 4015 (1988).
- [3] C. T. Chen, Y. Ma, and F. Sette, *Phys. Rev. A* **40**, 6737 (1989).
- [4] Y. Ma, C. T. Chen, G. Meigs, K. Randall, and F. Sette, *Phys. Rev. A* **44**, 1848 (1991).
- [5] K. Faegri, and H. Kelly, *Phys. Rev.* **19**, 1649 (1978).
- [6] M. Higashi, E. Hiroike, and T. Nakajima, *Chem. Phys.* **68**, 377 (1982).
- [7] M. Higashi, E. Hiroike, and T. Nakajima, *Chem. Phys.* **85**, 133 (1984).
- [8] C. Liegener, *Chem. Phys. Lett.* **106**, 201 (1984).
- [9] N. Correia, A. Flores-Riveros, H. Agren, K. Helenelund, L. Asplund, and U. Gelius, *J. Chem. Phys.* **83**, 2035 (1985); **83**, 2053 (1985).
- [10] A. Cesar, H. Agren, and V. Carravetta, *Phys. Rev. A* **40**, 187 (1989). See also A. Cesar and H. Agren, *Phys. Rev. A* **45**, 2833 (1992).
- [11] L. S. Cederbaum, P. Campos, F. Tarantelli, and A. Sgamellotti, *J. Chem. Phys.* **95**, 6634 (1991).
- [12] R. Colle and S. Simonucci, *Phys. Rev. A* **39**, 6247 (1989).
- [13] R. Colle and S. Simonucci, *Phys. Rev. A* **42**, 3913 (1990).
- [14] H. Agren, A. Cesar, and C. Liegener, *Adv. Quantum Chem.* **23**, 1 (1992).
- [15] F. K. Gel'mukhanov, L. N. Mazalov, A. V. Nikolaev, A. V. Kondratenko, V. G. Smirni, P. I. Wadash, and A. P. Sadvskii, *Dokl. Akad. Nauk SSSR* **225**, 597 (1975); F. K. Gel'mukhanov, L. N. Mazalov, and A. V. Kondratenko, *Chem. Phys. Lett.* **46**, 133 (1977).
- [16] W. Domcke and L. S. Cederbaum, *Phys. Rev. A* **16**, 1465 (1977).
- [17] F. Kaspar, W. Domcke, and L. S. Cederbaum, *Chem. Phys.* **44**, 33 (1979).
- [18] U. Fano, *Phys. Rev.* **124**, 1866 (1961).
- [19] W. Moddeman, T. Carlson, M. Krause, P. Pullen, W. Bull, and G. Schweitzer, *J. Chem. Phys.* **55**, 2317 (1971).
- [20] J. Kelber, D. Jennison, and R. Rye, *J. Chem. Phys.* **75**, 652 (1981).
- [21] L. Ungier and T. Thomas, *Chem. Phys. Lett.* **96**, 247 (1983).
- [22] H. Agren and H. Siegbahn, *Chem. Phys. Lett.* **72**, 498 (1981).
- [23] M. Larsson, B. J. Olsson, and P. Sigray, *Chem. Phys.* **139**, 457 (1989).
- [24] T. Aberg and G. Howat, in *Theory of the Auger Effect*, edited by S. Flügge and W. Melhorn, *Handbuch der Physik* Vol. 31 (Springer, Berlin, 1982).
- [25] D. P. Craig and T. Thirunamachandran, *Molecular Quantum Electrodynamics* (Academic, London, 1984).
- [26] R. Colle and S. Simonucci, in *Progress on Electronic Properties of Solids*, edited by R. Girlanda *et al.* (Kluwer, Amsterdam, 1989), p. 211.
- [27] R. Colle and S. Simonucci (unpublished).
- [28] F. B. Van Duyneveldt, IBM Report No. 16437, 1971 (unpublished); A. D. McLean, G. M. Low, and P. S. Berkowitz, *J. Mol. Spectrosc.* **64**, 184 (1977).
- [29] A. Golebiewski, and J. Mrozek, *Int. J. Quantum Chem.* **7**, 263 (1973); **7**, 1021 (1973).